Generation of a Wide-Band Electromagnetic Response Through a Laguerre Expansion Using Early-Time and Low-Frequency Data

Tapan K. Sarkar, *Fellow, IEEE,* and Jinhwan Koh

***Abstract*—The objective of this paper is to generate a wide-band and temporal response for three-dimensional conducting structures. This is accomplished through the use of a hybrid method that involves generation of early-time and low-frequency information for the electromagnetic structure of interest. These two, early-time and low-frequency information, are mutually complementary and contain all the necessary information for an ultrawide-band response for a sufficient record length. The time-domain response is modeled as a Laguerre series expansion. The frequency-domain response is also expressed in an analytic form using the same expansion coefficients used in modeling of the time-domain response. The data in both the domains is used to solve for the polynomials coefficients in a data-fitting procedure. Once the polynomial coefficients are known, the available data is simultaneously extrapolated in both domains. This approach is attractive because expansions with a few terms give good extrapolation in both time and frequency domains. The computation involved is minimal with this method.**

***Index Terms*—Early time, hybrid methods, Laguerre expansion, low frequency.**

I. Introduction

In ELECTROMAGNETIC analysis, field quantities are usually assumed to be time–harmonic. This suggests that the solution lies in the frequency domain. The method of moments (MOM), which uses an integral-equation formulation, can be used to perform the frequency-domain analysis. However, for broad-band analysis, this approach can get very computationally intensive; as the MOM program needs to be executed for each frequency of interest and, for high frequencies, the size of the matrix can be very large.

The time-domain approach is preferred for broad-band analysis. Other advantages of a time-domain formulation include easier modeling of nonlinear and time-varying media, and use of gating to eliminate unwanted reflections. For a time-domain integral-equation formulation, the method of marching on in time (MOT) is usually employed [1], [2]. A serious drawback of this algorithm is the occurrence of late-time instabilities in the form of high-frequency oscillation.

In this paper, we present a technique to overcome late-time oscillations. Using early-time and low-frequency data, we obtain stable late-time and broad-band information. A frequency-domain MOM approach can efficiently generate low-frequency data [3], while the MOT algorithm can be used to obtain stable early-time data quickly. Thus, the overall analysis is computationally very efficient.

The time and frequency-domain responses from three-dimensional conducting objects are considered in this paper. It is assumed that the conducting structures are excited by band-limited functions, such that both the time- and frequency-domain responses are of finite support for all practical purposes. From a strictly mathematical point-of-view, a causal time-domain response cannot be strictly band-limited and vice versa. However, a response strictly limited in time can be assumed to be approximately band-limited if the amplitude of the frequency response is too small (outside the region of interest) to be of any consequence.

In computational electromagnetics, one needs to obtain the electromagnetic "fingerprint" of an object. This is equivalent to obtaining the entire impulse response in the time domain or obtaining the transfer function over the entire frequency band. Both of these require tremendous computational resources. Here, we propose a hybrid approach, which will minimize the computational efforts. The goal is attained by generating early-time and low-frequency information that are not computationally demanding. A Laguerre series is then fit to the data in the time domain and its transform—a polynomial—in the frequency domain to extrapolate the response simultaneously both in time and frequency. In this approach, we are not creating any new information, but using the existing information to extrapolate the responses simultaneously in the time and frequency domains.

For these responses, an optimal choice of basis functions would, therefore, be one that provides compact support. The Laguerre series is well suited for real-life signals with compact support as it naturally enforces causality. The fact that the Fourier transform of Laguerre functions is an analytic function allows us to work simultaneously with time and frequency-domain data.

It is better to use the Laguerre polynomials instead of the associate Hermite functions [4], [5] even though the latter are the eigenfunctions of the Fourier transform operator. The problem with the Hermite expansion is that these polynomials are two sided $(-\infty, +\infty)$ and, hence, the origin of the expansion of the causal time-domain functions by a Hermite series is very critical. In contrast, the Laguerre series is defined only over the in-

Manuscript received January 14, 2000. This work was supported by the Office of Naval Research under Contract N00014-98-1-0279.

T. K. Sarkar is with the Department of Electrical Engineering and Computer Science, Syracuse University, Syracuse, NY 13244-1240 USA.

J. Koh is with the Department of Electronics and Electrical Engineering, Kyungpook National University, Taegu, Korea.

Publisher Item Identifier S 0018-9480(02)04053-X.

terval $[0, +\infty]$ and, hence, are considered to be more suited for the problem at hand, as they naturally enforce causality.

In Section II, we introduce the Laguerre functions and set up the relevant equations for the problem. In Section III, we discuss some numerical results. Finally, some conclusions are presented in Section IV.

II. Formulation

Consider the set of functions [6],

$$L_n(t) = \frac{1}{n!}\, e^x\, \frac{d^n\left(t^n e^{-t}\right)}{dt^n}, \qquad n \geq 0; \quad t \geq 0. \tag{1}$$

These are the Laguerre functions of order n. They are causal, i.e., exist for $t \geq 0$. They can also be computed in a stable fashion recursively through

$$\begin{aligned} L_0(t) &= 1 \\ L_1(t) &= 1 - t \\ L_n(t) &= \frac{2n-1-t}{n}\, L_{n-1}(t) - \frac{n-1}{n}\, L_{n-2}(t), \\ & \qquad n \geq 2; \quad t \geq 0. \end{aligned} \tag{2}$$

The Laguerre functions are orthogonal as

$$\int_0^\infty e^{-t} L_n(t) L_m(t)\, dt = \delta_m = \begin{cases} 1, & m = n \\ 0, & \text{otherwise.} \end{cases} \tag{3}$$

An orthonormal basis function set can be derived from the Laguerre functions through the representation

$$\phi_n(t, \ell) = e^{-t/2} L_n(t/\ell) \tag{4}$$

where ℓ is a scaling factor. A causal electromagnetic response function $x(t)$ at a particular location in space for $t \geq 0$ can be expanded into a Laguerre series as

$$x(t) = \sum_{n=0}^{\infty} a_n \phi_n(t, \ell_1). \tag{5}$$

Laguerre functions of order 0–3 are plotted in Fig. 1. These functions can approximate causal responses quite well and, by varying the scaling factor ℓ, the support provided by the expansion can be increased or decreased.

As can be seen, the Laguerre functions are causal and also their modality (number of local maximas and minimas) increases with the increase in order.

A signal with compact time support can be expanded as

$$x(t) = \sum_{n=0}^{N} a_n \phi_n(t, \ell_1). \tag{6}$$

The Fourier transform of the above expression can be evaluated as

$$X(f) = \sum_{n=0}^{N} \frac{a_n \left(-\frac{1}{2} + j\,\frac{f}{\ell_2}\right)^n}{2\pi\, d_2 \left(\frac{1}{2} + j\,\frac{f}{\ell_2}\right)^{n+1}} \tag{7}$$

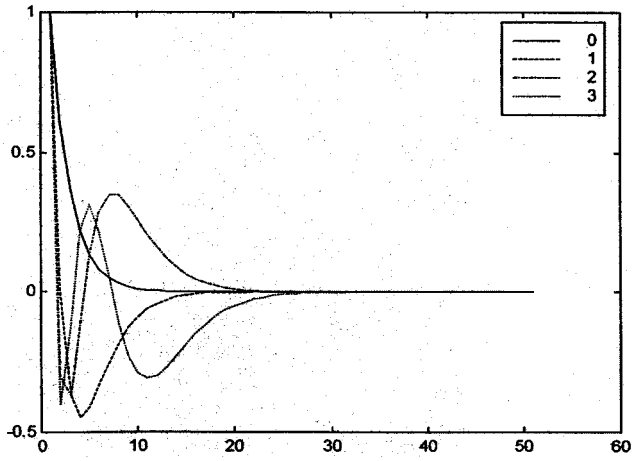

Fig. 1. Laguerre functions of order 0–3.

where $\ell_2 = (1/2\pi\ell_1)$ and $j = \sqrt{-1}$. The choice of the scaling factor ℓ_1 is crucial because it also affects ℓ_2 and these two decide the amount of support given by the Laguerre functions to the time- and frequency-domain responses, respectively. Given about 50%–60% of initial time-domain data and an equal amount of low-frequency data, with a proper choice of N (order of expansion) and ℓ_1 (scaling factor), it is possible to simultaneously extrapolate the function in both domains. The value of N can be decided by choosing a cutoff for the magnitude of the coefficients, i.e., discarding the ones that are smaller than a critical value. Choosing an unnecessarily large N will introduce oscillations in the extrapolation region. The coefficients for the Laguerre expansion are obtained by solving a total least-squares problem, using singular value decomposition (SVD) [7].

A. Matrix Formulation

Let M_1 and M_2 be the number of time- and frequency-domain samples that are given for the functions $x(t)$ and $X(f)$, respectively. Here, $X(f)$ is considered to be the Fourier transform of $x(t)$.

The matrix representation of the time-domain data, utilizing (6), would then be

$$\begin{bmatrix} \phi_0(t_1, \ell_1) & \phi_1(t_1, \ell_1) & \cdots & \phi_{N-1}(t_1, \ell_1) \\ \phi_0(t_2, \ell_1) & \phi_1(t_2, \ell_1) & \cdots & \phi_{N-1}(t_2, \ell_1) \\ \vdots & \vdots & \vdots & \vdots \\ \phi_0(t_{M_1}, \ell_1) & \phi_1(t_{M_1}, \ell_1) & \cdots & \phi_{N-1}(t_{M_1}, \ell_1) \end{bmatrix}_{M_1 \times N} \cdot \begin{bmatrix} a_0 \\ a_1 \\ \vdots \\ a_{N-1} \end{bmatrix}_{N \times 1} = \begin{bmatrix} x(t_1) \\ x(t_2) \\ \vdots \\ x(t_{M_1}) \end{bmatrix}_{M_1 \times 1}. \tag{8}$$

Similarly, the matrix representation in the frequency domain would be (9), shown at the bottom of the following page. By combining the two equations, we get (10), shown at the bottom of the following page. The N unknown coefficients of the expansion a_i are obtained by solving this matrix equation either

by using the iterative conjugate gradient method or the total least-squares implementation of the SVD.

III. Numerical Examples

In this section, five examples are presented to validate the above technique. A program to evaluate the currents on an arbitrarily shaped closed or open body using the electric-field integral equation (EFIE) is used [8]. The rationale for doing this is that we are going to use the EFIE both in the time [9] and frequency domains [8]. We utilize the same surface patching scheme for both domains, hence, eliminating some of the effects of discretization from this study. The triangular patching approximates the surface of a scatterer with a set of adjacent triangles. The current perpendicular to each nonboundary edge is an unknown to be solved for.

Although the program can be used with an arbitrary excitation, we used a linearly polarized plane wave with a Gaussian profile in time. The excitation has the form

$$\vec{E}^{\,\mathrm{inc}} = \vec{u}_i \frac{1}{\sigma\sqrt{\pi}} E_0 e^{-r^2} \tag{11}$$

$$\begin{bmatrix} \frac{1}{\frac{1}{2}+j\frac{f_1}{\ell_2}} & \frac{\left(-\frac{1}{2}+j\frac{f_1}{\ell_2}\right)}{\left(\frac{1}{2}+j\frac{f_1}{\ell_2}\right)^2} & \cdots & \frac{\left(-\frac{1}{2}+j\frac{f_1}{\ell_2}\right)^{N-1}}{\left(\frac{1}{2}+j\frac{f_1}{\ell_2}\right)^N} \\ \frac{1}{\frac{1}{2}+j\frac{f_2}{\ell_2}} & \frac{\left(-\frac{1}{2}+j\frac{f_2}{\ell_2}\right)}{\left(\frac{1}{2}+j\frac{f_2}{\ell_2}\right)^2} & \cdots & \frac{\left(-\frac{1}{2}+j\frac{f_2}{\ell_2}\right)^{N-1}}{\left(\frac{1}{2}+j\frac{f_2}{\ell_2}\right)^N} \\ \vdots & \vdots & \vdots & \vdots \\ \frac{1}{\frac{1}{2}+j\frac{f_{M_2}}{\ell_2}} & \frac{\left(-\frac{1}{2}+j\frac{f_{M_2}}{\ell_2}\right)}{\left(\frac{1}{2}+j\frac{f_{M_2}}{\ell_2}\right)^2} & \cdots & \frac{\left(-\frac{1}{2}+j\frac{f_{M_2}}{\ell_2}\right)^{N-1}}{\left(\frac{1}{2}+j\frac{f_{M_2}}{\ell_2}\right)^N} \end{bmatrix}_{M_2\times N} \begin{bmatrix} a_0 \\ a_1 \\ \vdots \\ a_{N-1} \end{bmatrix}_{N\times 1} = 2\pi\, d_2 \begin{bmatrix} X(f_1) \\ X(f_2) \\ \vdots \\ X(f_{M_2}) \end{bmatrix}_{M_2\times 1} \tag{9}$$

$$\begin{bmatrix} \phi_0(t_1,\ell_1) & \phi_1(t_1,\ell_1) & \cdots & \phi_{N-1}(t_1,\ell_1) \\ \phi_0(t_2,\ell_1) & \phi_1(t_2,\ell_1) & \cdots & \phi_{N-1}(t_2,\ell_1) \\ \vdots & \vdots & \vdots & \vdots \\ \phi_0(t_{M_1},\ell_1) & \phi_1(t_{M_1},\ell_1) & \cdots & \phi_{N-1}(t_{M_1},\ell_1) \\ \frac{1}{\frac{1}{2}+j\frac{f_1}{\ell_2}} & \frac{\left(-\frac{1}{2}+j\frac{f_1}{\ell_2}\right)}{\left(\frac{1}{2}+j\frac{f_1}{\ell_2}\right)^2} & \cdots & \frac{\left(-\frac{1}{2}+j\frac{f_1}{\ell_2}\right)^{N-1}}{\left(\frac{1}{2}+j\frac{f_1}{\ell_2}\right)^N} \\ \frac{1}{\frac{1}{2}+j\frac{f_2}{\ell_2}} & \frac{\left(-\frac{1}{2}+j\frac{f_2}{\ell_2}\right)}{\left(\frac{1}{2}+j\frac{f_2}{\ell_2}\right)^2} & \cdots & \frac{\left(-\frac{1}{2}+j\frac{f_2}{\ell_2}\right)^{N-1}}{\left(\frac{1}{2}+j\frac{f_2}{\ell_2}\right)^N} \\ \vdots & \vdots & \vdots & \vdots \\ \frac{1}{\frac{1}{2}+j\frac{f_{M_2}}{\ell_2}} & \frac{\left(-\frac{1}{2}+j\frac{f_{M_2}}{\ell_2}\right)}{\left(\frac{1}{2}+j\frac{f_{M_2}}{\ell_2}\right)^2} & \cdots & \frac{\left(-\frac{1}{2}+j\frac{f_{M_2}}{\ell_2}\right)^{N-1}}{\left(\frac{1}{2}+j\frac{f_{M_2}}{\ell_2}\right)^N} \end{bmatrix}_{(M_1+M_2)\times N} \begin{bmatrix} a_0 \\ a_1 \\ \vdots \\ a_{N-1} \end{bmatrix}_{N\times 1} = \begin{bmatrix} x(t_1) \\ x(t_2) \\ \vdots \\ x(t_{M_1}) \\ 2\pi d_2 X(f_1) \\ 2\pi d_2 X(f_2) \\ \vdots \\ 2\pi d_2 X(f_{M_2}) \end{bmatrix}_{(M_2+M_2)\times 1} \tag{10}$$

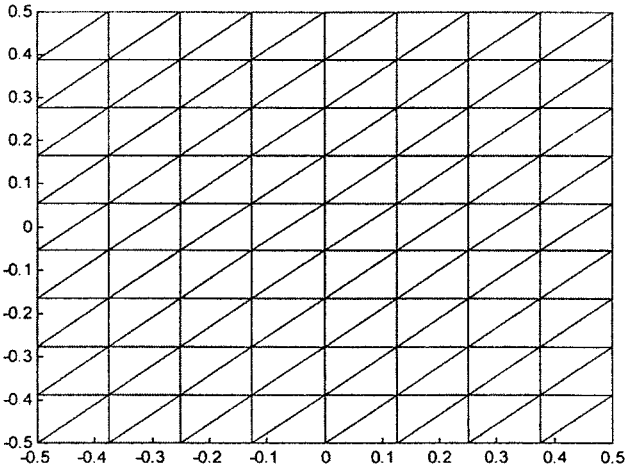

Fig. 2. Triangulation of a square plate.

where

$$\gamma = \frac{\left(t - t_0 - \vec{r} \cdot \vec{k}\right)}{\sigma} \tag{12}$$

- $\vec{u}_i$ unit vector that defines the polarization of the incoming plane wave;
- E_0 amplitude of the incoming wave;
- t_0 a delay, which is used so that the pulse rises smoothly from 0 for time $t < 0$ to its value at time t;
- $\vec{r}$ position of an arbitrary point in space;
- $\vec{k}$ unit wave vector defining the direction of arrival of the incident pulse;
- σ^2 spread factor of Gaussian input pulse.

To find the frequency response to the above Gaussian plane wave, the response of the system in the frequency domain is multiplied by the spectrum of the Gaussian plane wave. The spectrum is given by

$$F(j\omega) = \frac{E_0}{c} \exp\left(-\left[\frac{(\omega\sigma)^2}{4c^2} + j\omega t_0\right]\right), \qquad \omega = 2\pi f. \tag{13}$$

The electromagnetic responses are to be extrapolated from the currents induced on the parallel-plate resonator, plate sphere combination, resonating cavity, and a cone-hemisphere combination. All bodies are assumed to be perfectly conducting. Fig. 2 shows an example of the triangulation scheme used. It shows a plate being approximated by 144 triangles and 233 edges.

In all our computations, E_0 is chosen to be 377 V/m. The time step (Δt) is dictated by the discretization used in modeling the geometry of each example and is dictated by the highest frequency of operation. The frequency step (Δf) is 2 MHz. In all the examples, the extrapolated time-domain response is compared to the output of the time-domain response obtained from the MOT program [9] and the extrapolated frequency-domain response is compared to that of the MOM program [8]. In all the plots, dashed line refers to the extrapolated response using Laguerre expansions, while the solid line refers to the data obtained from the MOT or MOM programs.

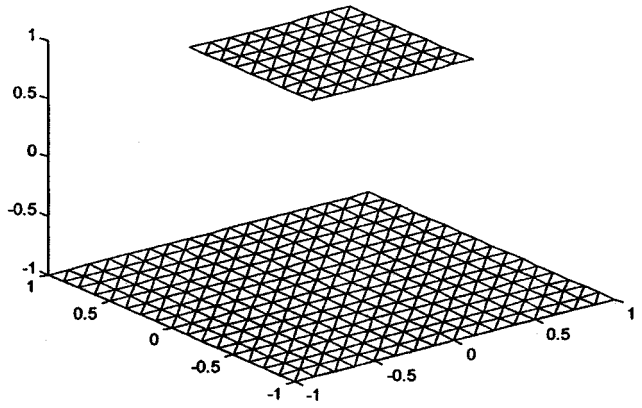

Fig. 3. Discretization of the two plates of unequal size.

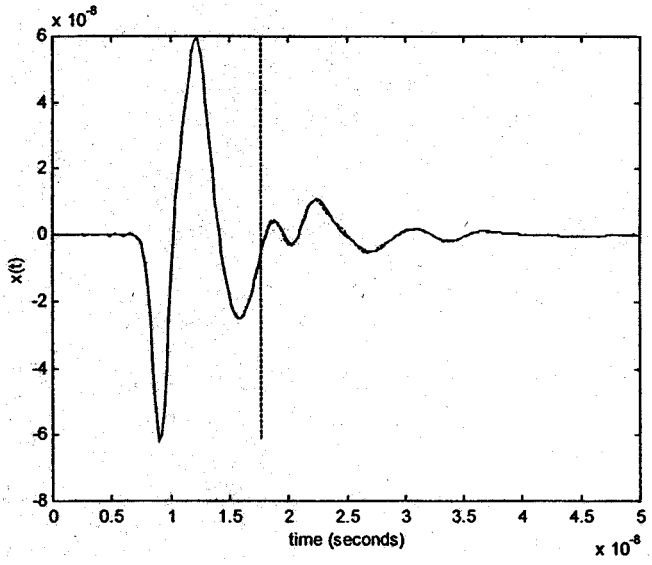

Fig. 4. Time-domain response at an edge on the smaller plate.

Example 1—Unequal Plates

In this example, we have two square plates of zero thickness and sides 1 and 2 m in the xy-plane. The configuration with the discretization is shown in Fig. 3. The plate separation is 2 m. The excitation arrives from the direction $\theta = 0°$, $\phi = 0°$, i.e., along the negative z-direction. $\vec{u}_i$ is along the x-axis. The time step used in the MOT program is 196.8 ps. In this example, $\sigma = 0.79$ ns and $t_0 = 9.2$ ns. The edge under consideration is on the smaller plate, in the y-direction, and is located at the center.

Using the MOT algorithm, time-domain data is obtained from $t = 0$ to $t = 50$ ns (250 data points). Also, frequency-domain data is obtained from dc to $f = 0.998$ GHz (500 data points). Assume that only the first 90 time-data points (up to $t = 18$ ns) and the first 120 frequency-data points (up to $f = 238$ MHz) are available. Solving for the matrix equation (10) using the available data, the polynomial coefficients are obtained. These coefficients are then used to extrapolate the time-domain response to 250 points (50 ns) and the frequency-domain response is extrapolated to 500 points (0.998 GHz).

The order of the expansion was chosen to be 60. From Fig. 4, it can be seen that the time-domain reconstruction is almost in-

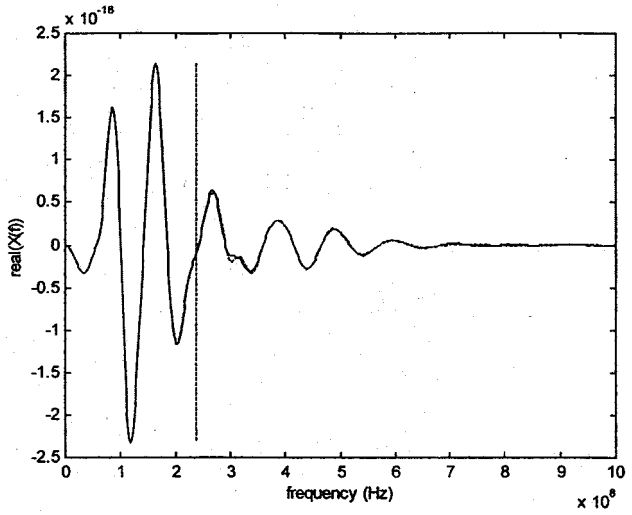

Fig. 5. Frequency response at the same edge located on the smaller plate—real part.

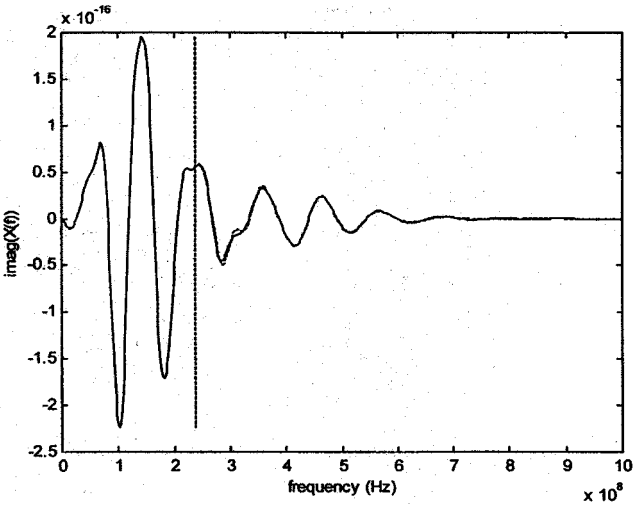

Fig. 6. Frequency response at the same edge located on the smaller plate—imag part.

distinguishable from the actual (MOT) data. The reconstruction in frequency domain is also very good, as can be seen from Figs. 5 and 6.

Example 2—Equal Plates

Two equal plates of side 1 m are placed as in the previous example, but the separation between the plates is reduced to 0.25 m so as to increase the resonance effects. The excitation arrives form the direction $\theta = 0°$, $\phi = 0°$, i.e., along the negative z-direction. $\vec{u}_i$ is along the x-axis. The time step used in the MOT program is 160.1 ps. In this example, $\sigma = 0.59$ ns and $t_0 = 2.30$ ns. The edge under consideration is in the y-direction and close to the center of the upper plate.

Using the MOT algorithm, the time-domain data is obtained from $t = 0$ to $t = 124.8$ ns (780 data points). Also, frequency-domain data is obtained from dc to $f = 1.558$ GHz (780 data points). Assume that only the first 70 time-data points (up to $t = 11.05$ ns) and first 90 frequency-data points (up to $f = 178$ MHz) are available. Solving for the matrix equation

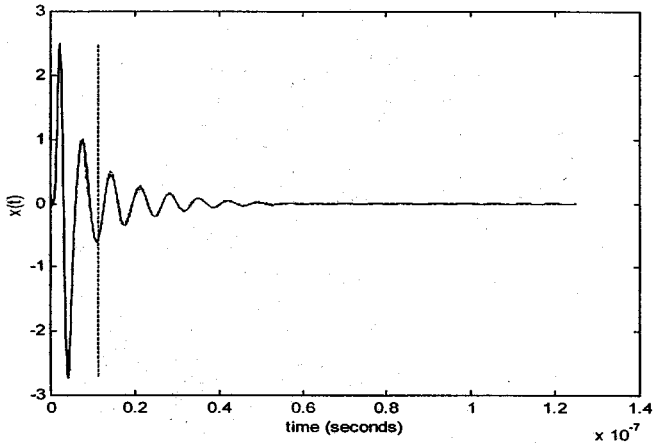

Fig. 7. Time-domain response at one of the edges on the upper plate.

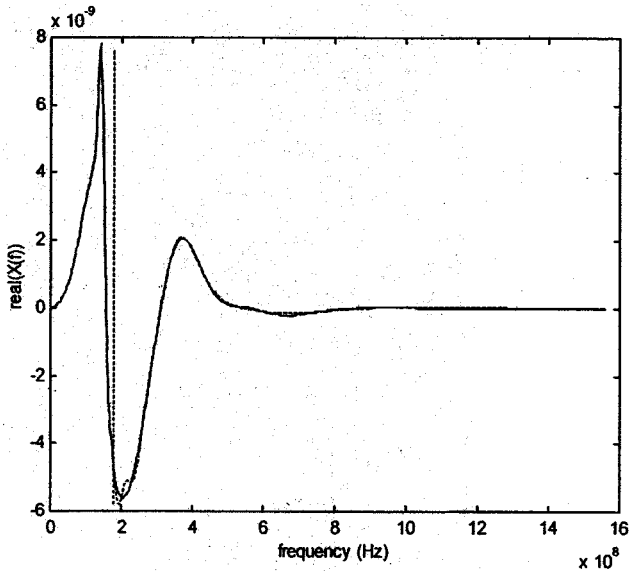

Fig. 8. Frequency response at one of the edges on the upper plate—real part.

(10) using the available data, the time-domain response is extrapolated to 780 points (124.8 ns) and the frequency-domain response is extrapolated to 780 points (1.558 GHz).

The order of the expansion was chosen to be 40. From Fig. 7, it can be seen that the time-domain reconstruction is almost indistinguishable from the actual (MOT) data. The reconstruction in frequency domain also agrees closely with actual (MOM) data, as can be seen from Figs. 8 and 9.

Example 3—Plate–Sphere

1) Separation of 5 m: A plate–sphere combination is considered next, with the sphere of radius 1 m centered at the origin and separation of 5 m. The actual discretization is shown in Fig. 10. The excitation arrives from $\theta = (\pi/2)$, $\phi = 0°$ i.e., along the negative x-direction. $\vec{u}_i$ is along the x-axis. In this example, $\sigma = 2.359$ ns and $t_0 = 9.20$ ns. The time step used in the MOT program is 0.484 ns. The edge under consideration is on the plate, along the y-direction, and close to the center.

The time-domain data is obtained using the MOT algorithm from $t = 0$ to $t = 145$ ns (300 data points). Also, the frequency-domain data is obtained using the MOM program from dc to

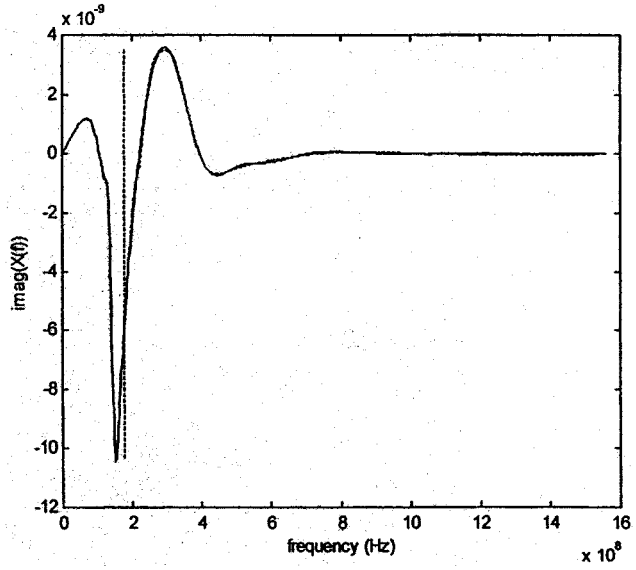

Fig. 9. Frequency response at one of the edges on the upper plate—imag part.

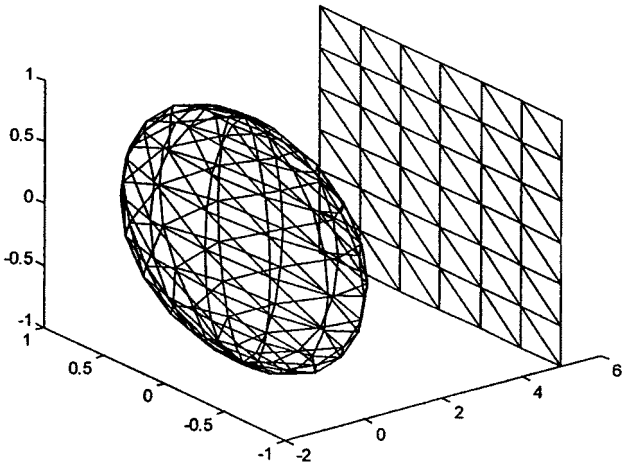

Fig. 10. Discretization of the plate–sphere structure.

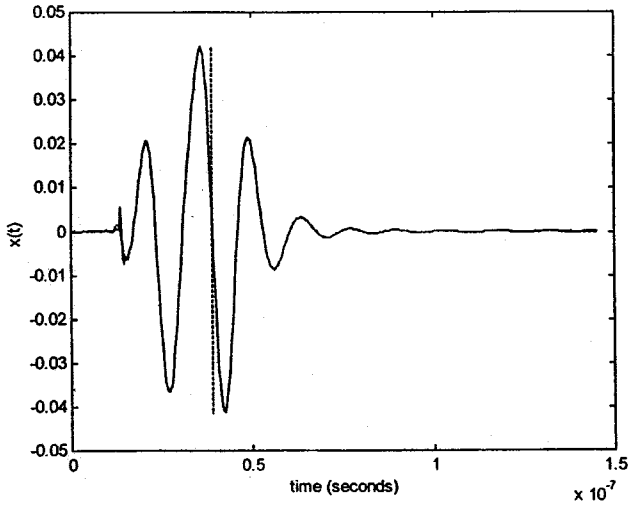

Fig. 11. Time-domain response at one of the edges on the plate, 5-m separation.

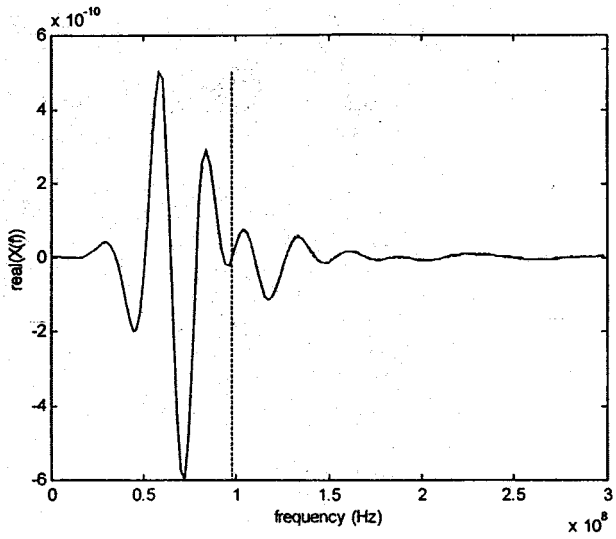

Fig. 12. Frequency response at one of the edges on the plate—real part, 5-m separation.

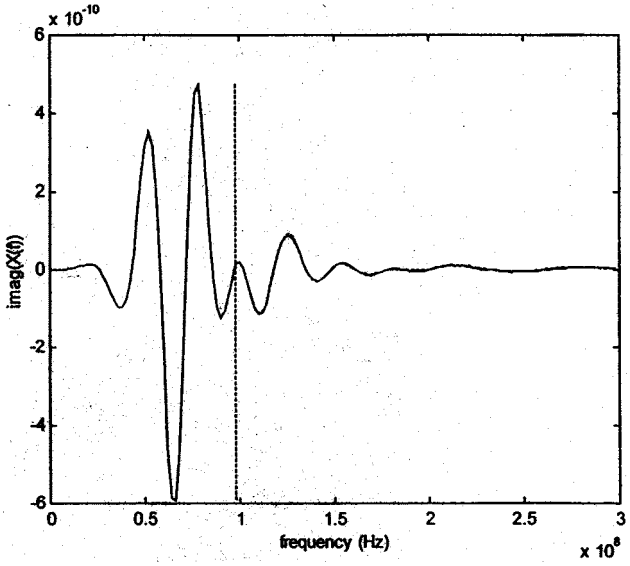

Fig. 13. Frequency response at one of the edges on the plate—imag part, 5-m separation.

$f = 298$ MHz (150 data points). Using the first 80 time data points (up to 38.67 ns) and the first 50 frequency data points (up to 98 MHz), the time-domain response is extrapolated to 300 points, and the frequency-domain response is extrapolated to 150 points.

The order of the expansion is chosen to be 50. From Fig. 11, it can be seen that the time-domain reconstruction is agreeable to the actual MOT data. From Figs. 12 and 13, the real and imaginary parts also have reasonably good reconstruction using the Laguerre expansions.

2) Separation of 12 m: The separation between the plates is increased to 12 m. All the other parameters are kept unchanged.

The time-domain data is obtained using the MOT algorithm from $t = 0$ to $t = 145$ ns (300 data points). Also, the frequency-domain data is obtained using the MOM program from dc to $f = 298$ MHz (150 data points). Using the first 130 time data points (up to 62.4 ns) and first 50 frequency data points (up to 98 MHz), the time-domain response is extrapolated to 300 points and the frequency-domain response is extrapolated to 150 points.

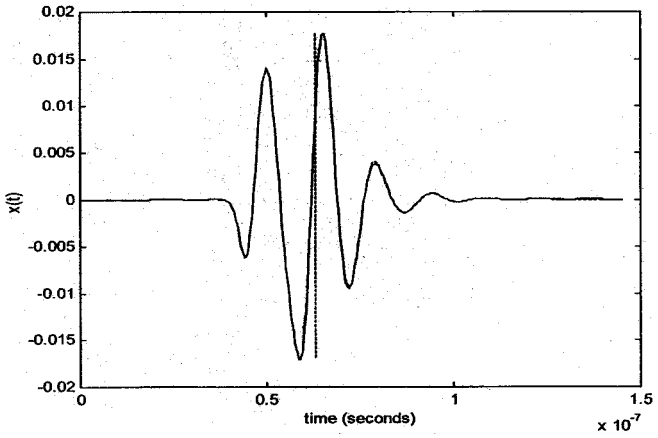

Fig. 14. Time-domain response at one of the edges on the plate, 12-m separation.

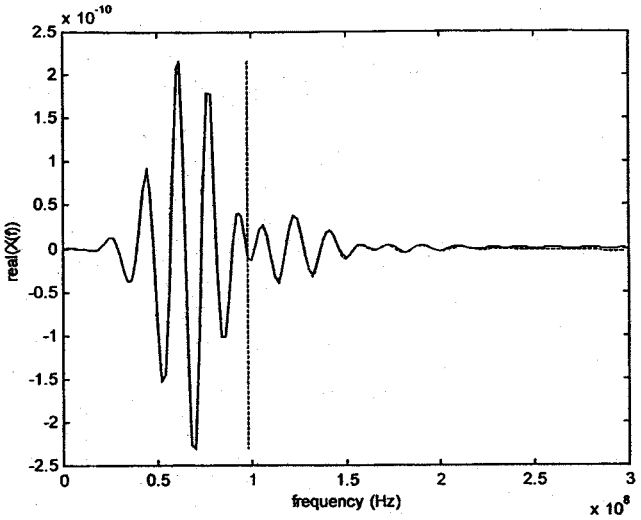

Fig. 15. Frequency response at one of the edges on the plate—real part, 12-m separation.

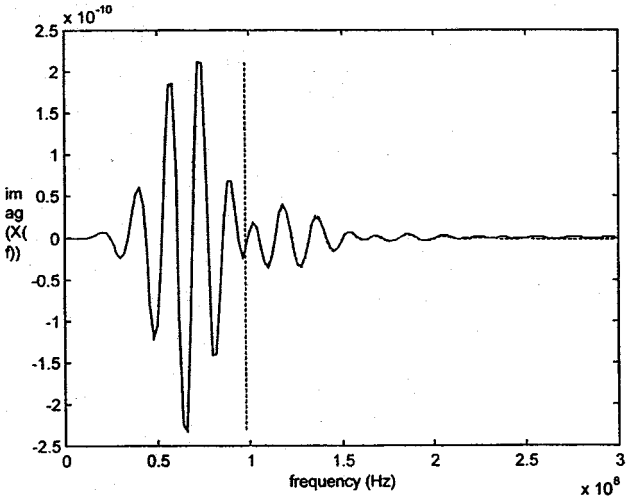

Fig. 16. Frequency response at one of the edges on the plate—imag part, 12-m separation.

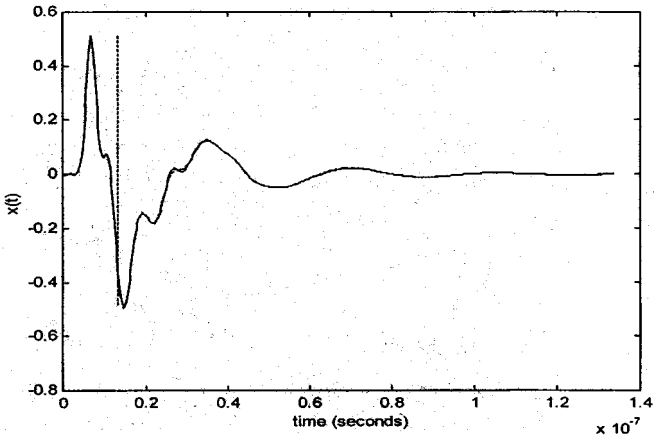

Fig. 17. Time-domain response at one of the edges in the cavity.

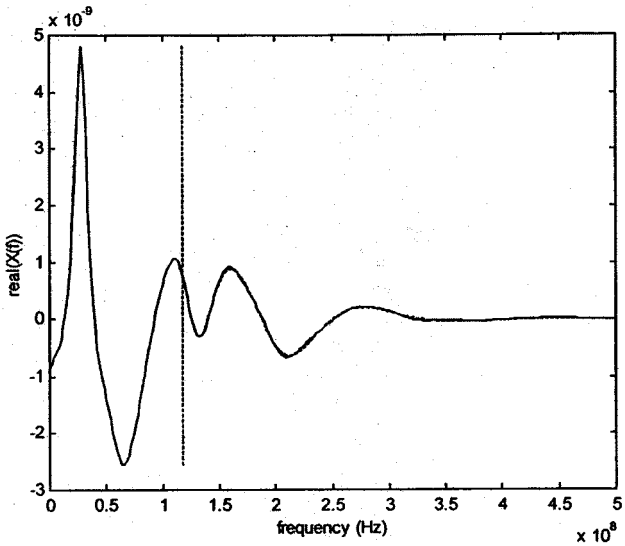

Fig. 18. Frequency-domain response at the same edge in the cavity—real part.

The order of the expansion is chosen to be 70. From Fig. 14, it can be seen that the time-domain reconstruction is agreeable to the actual MOT data. From Figs. 15 and 16, the real and imaginary parts also have reasonably good reconstruction using the Laguerre expansions.

Example 4—Cavity

In this example, a rectangular cavity of dimensions 1 m $\times$ 1 m $\times$ 4 m, centered at the origin with its faces lined up along the three coordinate axes and its length along the x-axes is considered. The face at $x = 4$ m is open. The excitation arrives from the direction $\theta = (5\pi/6)$, $\phi = (\pi/6)$, and $\vec{u}_i$ is along $\theta = (\pi/6)$, $\phi = (5\pi/6)$. In this example, $\sigma = 1.18$ ns and $t_0 = 4.56$ ns. The time step used in the MOT program is 0.267 ns.

The time-domain data is obtained using the MOT algorithm from $t = 0$ to $t = 133.33$ ns (500 data points). Also, the frequency-domain data is calculated with the MOM program from dc to $f = 498$ MHz (250 data points). Assuming that the first 50 time data points (up to $t = 13.33$ ns) and first 60 frequency data points (up to $f = 118$ MHz) are available, the time-domain response was extrapolated to 500 points and the frequency-domain response was extrapolated to 250 points. N was chosen to be 40. From Fig. 17, it can be seen that time-domain response closely agrees with the actual MOT data. The frequency-domain reconstruction is also close from Figs. 18 and 19.

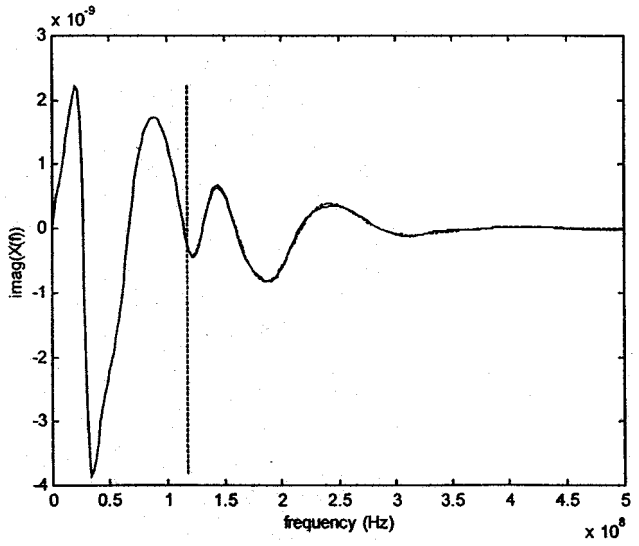

Fig. 19. Frequency-domain response at the same edge in the cavity—imag part.

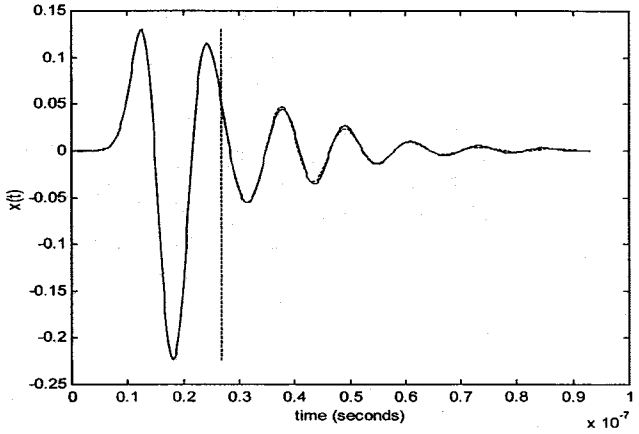

Fig. 20. Time-domain response at one of the edges on a cone–hemisphere.

Example 5—Cone–Hemisphere

In this example we have a combination of a cone and hemisphere, with the hemisphere attached to the base of a cone and its axis oriented along the x-direction. The bases of the cone and hemisphere have a radius 1 m and the height of the cone is 4 m. The excitation arrives from the direction $\phi = 0°$, $\theta = 0°$, i.e., along the negative z-direction. $\vec{u}_i$ is along the y-axis. In this example, $\sigma = 2.948$ ns and $t_0 = 11.495$ ns. The time step used is 206.67 ps and the frequency step is 2 MHz. The time-domain response is calculated using the MOT algorithm from $t = 0$ to $t = 93$ ns (450 data points). Also, the frequency-domain response is calculated with the MOM program from dc to $f = 448$ MHz (225 data points). Assuming that the first 130 time data points (up to $t = 26.66$ ns) and the first 40 frequency data points (up to $f = 78$ MHz) are available, the time-domain response was extrapolated to 450 points and the frequency-domain response is extrapolated to 225 points. N was chosen to be 40. From Fig. 20, it can be seen that the time-domain response closely agrees with the actual MOT data. The frequency-domain reconstruction is also close, as seen from Figs. 21 and 22.

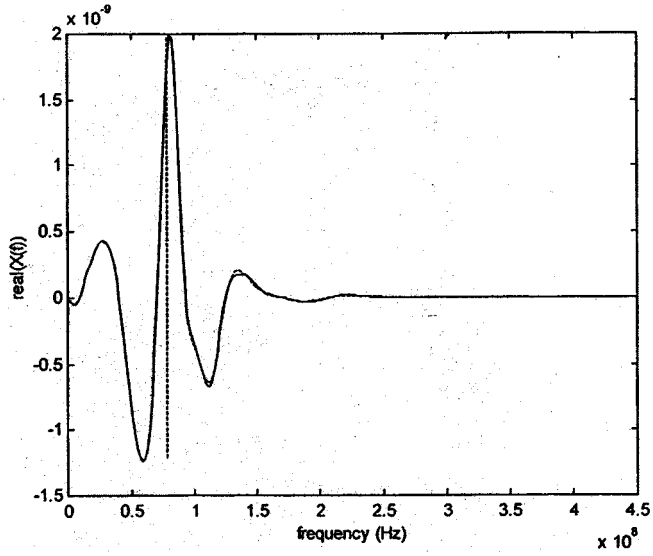

Fig. 21. Frequency-domain response at the same edge on a cone–hemisphere—real part.

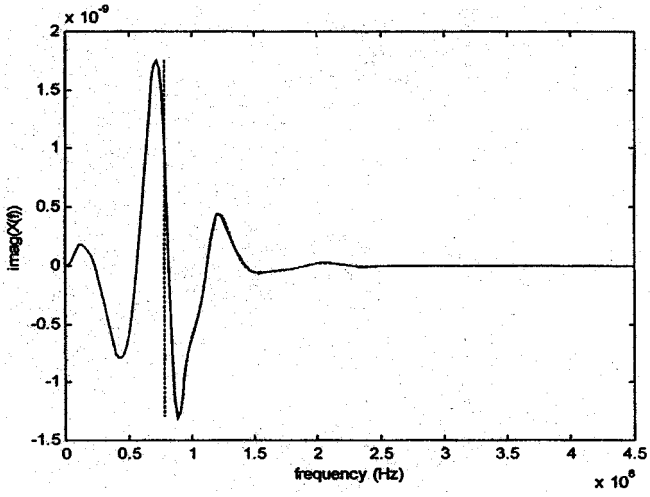

Fig. 22. Frequency-domain response at the same edge on a cone–hemisphere—imag part.

IV. Conclusions

This paper deals with the problem of simultaneous extrapolation in time and frequency domains using only early-time and low-frequency data. This has been accomplished through the use of Laguerre expansion, which are inherently causal and, thus, fit the time-domain data better than the associate Hermite functions. The computation involved is minimal because we require only early-time and low-frequency information. In addition, we need to solve a small matrix equation. This, coupled with the fact that expansions of order around 50 give good representation of the signals in both domains, ensures that this method is computationally very efficient.

In this paper, we have applied this technique to the problem of extrapolating the current on a scatterer being excited by a uniform plane wave. Six examples were considered—parallel-plate resonator, plate–sphere combination, resonating cavity, and a

cone–hemisphere combination. Using early-time and low-frequency data, we have demonstrated the possibility of good extrapolation in both the time and frequency domains.

There are several issues that are yet to be answered for this approach. One is the question of sensitivity and the second is the order of the polynomial required. These issues will be addressed in the future.

REFERENCES

[1] R. S. Adve, T. K. Sarkar, O. M. Pereira-Filho, and S. M. Rao, "Extrapolation of time domain responses from three dimensional conducting objects utilizing the matrix pencil technique," *IEEE Trans. Antennas Propagat.*, vol. 45, pp. 147–156, Jan. 1997.

[2] Y. Hua and T. K. Sarkar, "Matrix pencil method for estimating parameters of exponentially damped/undamped sinusoids in noise," *IEEE Trans. Signal Processing*, vol. 38, pp. 814–824, May 1990.

[3] S. Narayana, T. K. Sarkar, and R. S. Adve, "A comparison of two techniques for the interpolation/extrapolation of frequency domain responses," *Digital Signal Processing*, vol. 6, no. 1, pp. 51–67, Jan. 1996.

[4] T. K. Sarkar and O. M. Pereira-Filho, "Using the matrix pencil method to estimate the parameters of a sum of complex exponentials," *IEEE Antennas Propagat. Mag.*, vol. 37, pp. 48–55, Feb. 1995.

[5] M. M. Rao, T. K. Sarkar, T. Anjali, and R. S. Adve, "Simultaneous extrapolation in time and frequency domains using Hermite expansion," *IEEE Trans. Antennas Propagat.*, vol. 47, pp. 1108–1115, June 1999.

[6] A. D. Poularikas, *The Transforms and Applications Handbook*. Piscataway, NJ: IEEE Press, 1996.

[7] G. H. Golub and C. F. Van Loan, *Matrix Computations*. Baltimore, MD: The Johns Hopkins Univ. Press, 1991.

[8] B. M. Kolundzjia, J. S. Ognjanovic, T. K. Sarkar, and R. F. Harrington, *WIPL, Software for Electromagnetic Modeling of Composite Wire and Plate Structures*. Norwood, MA: Artech House, 1995.

[9] D. A. Vechinski, S. M. Rao, and T. K. Sarkar, "Transient scattering from three dimensional arbitrarily shaped dielectric bodies," *J. Opt. Soc. Amer. A, Opt. Image Sci.*, vol. 11, no. 4, pp. 1458–1470, 1994.

Tapan K. Sarkar (S'69–M'76–SM'81–F'92) received the B.Tech degree from the Indian Institute of Technology, Kharagpur, India, in 1969, the M.Sc.E. degree from the University of New Brunswick, Fredericton, NB, Canada, in 1971, and the M.S. and Ph.D. degrees from Syracuse University, Syracuse, NY, in 1975.

From 1975 to 1976, he was with the TACO Division, General Instruments Corporation, Sherburne, NY. From 1976 to 1985, he was with the Rochester Institute of Technology, Rochester, NY. From 1977 to 1978, he was a Research Fellow at the Gordon McKay Laboratory, Harvard University, Cambridge, MA. He is currently a Professor in the Department of Electrical and Computer Engineering, Syracuse University, Syracuse, NY. He has authored or co-authored over 210 journal papers and numerous conference papers and has authored chapters in 28 books. He has authored ten books, including *Iterative and Self Adaptive Finite-Elements in Electromagnetic Modeling* (Norwood, MA: Artech House, 1998). He is on the Editorial Board of *Journal of Electromagnetic Waves and Applications* and *Optical Technology Letters*. His current research interests deal with numerical solutions of operator equations arising in electromagnetics and signal processing with application to system design.

Dr. Sarkar is a Registered Professional Engineer in the State of New York. He is a member of Sigma Xi and the International Union of Radio Science (URSI) Commissions A and B. He was an associate editor for feature papers of the *IEEE Antennas and Propagation Society Newsletter* and the Technical Program chairman for the 1988 IEEE Antennas and Propagation Society (IEEE AP-S) International Symposium and URSI Radio Science Meeting. He was appointed the U.S. Research chairman for to many URSI General Assemblies. He was the chairman of the Intercommission Working Group of International URSI on Time-Domain Metrology (1990–1996). He was the recipient of the 1977 Best Solution Award presented at the Rome Air Development Center (RADC) Spectral Estimation Workshop and the Best Paper Award of the IEEE TRANSACTIONS ON ELECTROMAGNETIC COMPATIBILITY in 1979 and at the 1997 National Radar Conference. He was the recipient of the 1996 College of Engineering Research Award and the Chancellor's Citation for Excellence in Research, Syracuse University. He was also the recipient of the title of *Docteur Honoris Causa* from the Universite Blaise Pascal, Clermont Ferrand, France, in 1988 and the Medal of the City Clermont Ferrand, France, in 2000.

Jinhwan Koh was born in Taegu, Korea. He received the B.S. degree in electronics from Inha University, Inchon, Korea, and the M.S. and Ph.D. degrees in electrical engineering from Syracuse University, Syracuse, NY, in 1997 and 1999, respectively.

He was with the Goldstar Electron Semiconductor Company, Seoul, Korea. He is currently a Professor in the Department of Electronics and Electrical Engineering, Kyungpook National University, Taegu, Korea. His current research interests include digital signal processing related to adaptive antenna problems and data restoration.